J Neural Transm (2013) 120:375–382
DOI 10.1007/s00702-012-0906-8

TRANSLATIONAL NEUROSCIENCES - ORIGINAL ARTICLE

Region-specific causal mechanism in the effects of ammonia on cerebral glucose metabolism in the rat brain

Nobuyuki Maruoka · Tetsuhito Murata · Naoto Omata · Hironori Mitsuya · Yasushi Kiyono · Hidehiko Okazawa · Yuji Wada

Received: 29 July 2012 / Accepted: 16 October 2012 / Published online: 4 November 2012

Abstract Ammonia, which is considered to be the main agent responsible for hepatic encephalopathy, inhibits oxidative glucose metabolism in the brain. However, the effects of ammonia on cerebral glucose metabolism in different brain regions remains unclear. To clarify this issue, we added ammonia directly to fresh rat brain slices and measured its effects on glucose metabolism. Dynamic positron autoradiography with [^{18}F]2-fluoro-2-deoxy-D-glucose and 2-(4-iodophenyl)-3-(4-nitrophenyl)-5-(2,4-disulfophenyl)-2H-tetrazolium (WST-1) colorimetric assay revealed that ammonia significantly increased the cerebral glucose metabolic rate and depressed mitochondrial function, as compared to the unloaded control in each of the brain regions examined (cerebral cortex, striatum, and cerebellum), reflecting increased glycolysis that compensates for the decrease in aerobic metabolism. Pre-treatment with (+)-5-methyl-10,11-dihydro-5H-dibenzo[a,d]cyclohepten-5,10-imine hydrogen maleate (MK-801), a *N*-methyl-D-aspartate (NMDA) receptor antagonist, significantly attenuated these changes induced by ammonia in cerebellum, but not in cerebral cortex or striatum. The addition of ammonia induced an increase in cyclic guanosine monophosphate (cGMP) levels in cerebellum, but not in cerebral cortex or striatum, reflecting the activation of the NMDA receptor-nitric oxide-cGMP pathway. These results suggested that NMDA receptor activation is responsible for the impairment of glucose metabolism induced by ammonia specifically in cerebellum.

Keywords Ammonia · Brain slice · [^{18}F]2-fluoro-2-deoxy-D-glucose · Glucose metabolism · Hepatic encephalopathy · *N*-methyl-D-aspartate

N. Maruoka (✉) · T. Murata · N. Omata · H. Mitsuya · Y. Wada
Department of Neuropsychiatry, University of Fukui, Fukui, Japan
e-mail: maruoka@u-fukui.ac.jp

Y. Kiyono · H. Okazawa
Biomedical Imaging Research Center, University of Fukui, Fukui, Japan

Introduction

Ammonia is a product of degradation of compounds such as proteins. It is toxic at high concentrations, leading to functional disturbances in the central nervous system. Ammonia is thought to be the main agent responsible for the neurological alterations in patients with hepatic encephalopathy caused by liver failure. However, the molecular mechanism of the neurological alterations by ammonia remains unclear.

Ammonia is reported to impair respiratory energy metabolism. High concentrations of ammonia inhibit cerebral oxidative metabolism, resulting in depression of ATP levels (Izumi et al. 2005). There are at least two mechanisms that contribute to the effects of ammonia on energy metabolism. First, *N*-methyl-D-aspartate (NMDA) receptor antagonists limit the depression of brain ATP levels induced by ammonia (Kosenko et al. 1994), which suggests the importance of NMDA receptor activation. Second, ammonia inhibits α-ketoglutarate dehydrogenase (αKGDH), an enzyme required for ATP generation in the tricarboxylic acid (TCA) cycle (Lai and Cooper 1986). In the presence of ammonia, α-ketoglutarate and pyruvate accumulate, which suggests that ammonia inhibits the TCA cycle in the brain (McKhann and Tower 1961). These changes help to explain the decline in the cerebral metabolic rate for oxygen observed in patients with hepatic encephalopathy (Aggarwal et al. 2005).

Although it is widely agreed that ammonia inhibits oxidative energy metabolism, no studies have been undertaken to investigate the effects of ammonia on cerebral glucose metabolism in different brain regions.

For imaging of live brain slices, we developed the "dynamic positron autoradiography technique" (dPAT), which utilizes positron emitter-labeled ligands as probes and a radioluminography plate as a detector (Murata et al. 1999; Omata et al. 2000). Serial two-dimensional images of radioactivity in brain tissue slices can be constructed quantitatively with a short exposure time while they are still alive in the incubation solution, due to the high specific radioactivity of the radiotracers, high energy of positrons, and high sensitivity of the radioluminography plate. The dPAT is particularly useful for examining the effect of ammonia itself on cerebral glucose metabolism because ammonia and other agents can be applied directly to brain slices with precisely controlled concentrations at specific time intervals.

In the present study, we added ammonia directly to fresh rat brain slices and serially measured the dynamic changes in the cerebral metabolic rate for glucose (CMRglc) produced by ammonia using the dPAT with [^{18}F]2-fluoro-2-deoxy-D-glucose ([^{18}F]FDG) as a tracer. In addition, to clarify how NMDA receptor activation is involved in the promotion of the metabolic disturbance, we quantitatively evaluated the effects of the addition of (+)-5-methyl-10,11-dihydro-5H-dibenzo[a,d]cyclohepten-5,10-imine hydrogen maleate (MK-801) as an NMDA receptor antagonist on the ammonia-induced changes in cerebral glucose metabolism.

Activation of the NMDA receptor leads to increased intracellular calcium levels. Calcium binds to calmodulin, which activates neuronal nitric oxide synthase (NOS), increasing the formation of nitric oxide (NO), which in turn activates soluble guanylate cyclase and increases cyclic guanosine monophosphate (cGMP) (Hermenegildo et al. 2000). Since it is widely accepted that this signal transduction pathway is activated in acute hyperammonemia (Felipo and Butterworth 2002), we also measured activation of the NMDA receptor-NO-cGMP pathway in rat brain slices.

Materials and methods

Dynamic positron autoradiography technique (dPAT)

All animal procedures were approved by the Animal Care and Use Committee of the University of Fukui. Male Wistar rats (250–300 g) were decapitated and their brains were quickly removed. Sagittal brain slices (300 μm in thickness; $n = 24$) were prepared from eight animals with a microslicer (DTK-2000, Dosaka EM, Kyoto, Japan) and incubated as previously described (Murata et al. 1999; Omata et al. 2000). Each of the brain slices included three regions of interest (cerebral cortex, striatum, and cerebellum). The setup for incubation of the slices was composed of double polystyrene chambers (outer and inner ones). The outer chamber was filled with 80 ml of Krebs–Ringer solution (in mM: NaCl, 124; KCl, 5; $MgCl_2$, 1; $CaCl_2$, 2; KH_2PO_4, 1.2; $NaHCO_3$, 26; glucose, 10) and the inner chamber was immersed in it. The bottom of the inner chamber was made of a nylon net, and the bottom of the outer chamber was a 10 μm thick polyvinylidene chloride film that was penetrable to beta and gamma rays of ^{18}F. The prepared slices were placed in the inner chamber and were covered with a 300 μm thick stainless steel ring as the upper side was braced by a nylon net. During the incubation, Krebs–Ringer solution was maintained at 36 °C and continuously bubbled with 95 % O_2/5 % CO_2 gas to promote consistent perfusion within the chamber. ^{18}F was produced by ^{18}O (p,n) ^{18}F nuclear reactions, and [^{18}F]FDG was produced by the method of Hamacher et al. (1986) using an automated [^{18}F]FDG synthesis system (NKK Co. Ltd, Tokyo, Japan). The specific radioactivity of [^{18}F]FDG was 1–2 Ci/mmol at the end of the synthesis, and the total concentration (labeled plus unlabeled) used in the experiments was 0.54–1.09 μg/ml (3.0–6.0 μM). After 1 h of pre-incubation, the slices were incubated in Krebs–Ringer solution containing [^{18}F]FDG diluted to 150 kBq/ml. The double polystyrene chambers were put on the radioluminography plates (BAS-MP 2040S, Fuji Photo Film Co., Tokyo, Japan), and the exposed plates were scanned using an FLA-7000 bio-imaging system (Fuji Photo Film Co.).

A three-compartment model using the Gjedde–Patlak graphical method was applied to the image data for determination of the net influx constant of [^{18}F]FDG (= K, proportional to the CMRglc) (Murata et al. 1999; Omata et al. 2000). The Gjedde–Patlak graphical method (Gjedde 1981; Patlak et al. 1983) is based on the following equation in the equilibrium state (Sokoloff et al. 1977; Huang et al. 1980):

$$\mathrm{Ci}^*(t)/\mathrm{Cp}^*(t) = K \cdot \int_0^t \mathrm{Cp}^*(\tau)\mathrm{d}\tau/\mathrm{Cp}^*(t) + V$$

where Ci*(t), which represents the sum of Ce*(t) ([^{18}F]FDG in tissue) and Cm*(t) ([^{18}F]FDG-6-PO_4 in tissue), is the total brain tissue radioactivity, Cp*(t) ([^{18}F]FDG in bathing medium) is the input function, and V is related to the effective distribution volume of the tracer [^{18}F]FDG. Therefore, K is estimated from the slope of the linear portion of the graph, Ci*(t)/Cp*(t) (Y-axis) versus Cp*(t)dt/Cp*(t) (X-axis). The rate of delivery of the tracer to the brain slices is determined by the diffusion rate, because of the presence of [^{18}F]FDG at a certain concentration in the

medium, without interference by blood-borne factors (the product of cerebral perfusion rate and extraction fraction, as in the living brain). Therefore, the slope does not have the units of the net influx constant defined by Gjedde–Patlak (K, ml/g per min) (Gjedde 1981; Patlak et al. 1983) but is a fractional rate constant for phosphorylation of [^{18}F]FDG (k_3*, min^{-1}) (Murata et al. 1999; Omata et al. 2000).

Twenty-four slices were divided into four groups: the control ($n = 6$); ammonia-treated group ($n = 6$); ammonia- and MK-801-treated group ($n = 6$); MK-801-treated group ($n = 6$). Two-hundred minutes after addition of [^{18}F]FDG, ammonium chloride (10 mM) was loaded and its effects were evaluated using linear regression analysis to calculate the slopes (= k_3*) from the Gjedde–Patlak plot under each equilibrium state. MK-801 (100 μM) was dissolved in the vehicle (ethanol) and added at 170 min (i.e. 30 min prior to ammonia loading), and its effect on the slope (= k_3*) was evaluated. The final concentration of the vehicle in the incubation medium was 1 %. Control slices were treated with the vehicle alone, which had no effect on [^{18}F]FDG uptake at the final concentration.

Determination of mitochondrial function

To assess mitochondrial function, mitochondrial dehydrogenase (succinate-tetrazolium reductase) activity was determined using the 2-(4-iodophenyl)-3-(4-nitrophenyl)-5-(2,4-disulfophenyl)-2H-tetrazolium (WST-1) colorimetric assay (Roche Diagnostics, Indianapolis, IN, USA). WST-1 is a tetrazolium dye containing an electron-coupling reagent that is cleaved by mitochondrial dehydrogenase to produce formazan, a dark red dye. For these studies, 24 slices from 8 animals which were different from those used in the aforementioned experiments were divided into four groups: the control ($n = 6$); ammonia-treated group ($n = 6$); ammonia- and MK-801-treated group ($n = 6$); MK-801-treated group ($n = 6$). Brain slices were incubated for 5 h in 80 ml of Krebs–Ringer solution containing ammonia in the same equipment used in the dPAT. 8 ml of WST-1 was added 2 h after ammonia loading. MK-801 (100 μM) was added 30 min prior to ammonia loading, and its effect was evaluated. After incubation, the slices were trimmed down with razor blades and separated to the desired regions (cerebral cortex, striatum, and cerebellum). Then the trimmed samples were weighed and homogenized in cold 10× phosphate-buffered saline using an ultrasonic disrupter (UR-20P, Tomy Seiko Co. Ltd, Tokyo, Japan) to give a 50 % (w/v) homogenate. Each homogenate was centrifuged at 12,000g and 4 °C for 3 min. The supernatant was used for the measurement of absorbance at 450 nm, which reflects the concentration of WST-1-formazan (product of WST-1 reduction). Control slices were treated with the vehicle alone, which had no effect on this assay at the final concentration (1 %).

Determination of cGMP content

For these studies, 24 slices from 8 animals which were different from those used in the aforementioned experiments were divided into four groups: the control ($n = 6$); ammonia-treated group ($n = 6$); ammonia- and MK-801-treated group ($n = 6$); MK-801-treated group ($n = 6$). Brain slices were incubated for 5 h in 80 ml of Krebs–Ringer solution containing ammonia in the same equipment as that used in the dPAT. MK-801 (100 μM) was administered 30 min prior to ammonia loading, and its effect was evaluated. After incubation, the slices were trimmed down with razor blades and separated to the desired regions (cerebral cortex, striatum, and cerebellum). Then the trimmed samples were weighed and homogenized in cold 6 % (w/v) trichloroacetic acid using an ultrasonic disrupter (UR-20P, Tomy Seiko Co. Ltd, Tokyo, Japan) to give a 10 % (w/v) homogenate. Each homogenate was centrifuged at 2,000g and 4 °C for 15 min. The supernatant was washed four times with five volumes of water-saturated diethyl ether. The aqueous extract remaining was dried, and then used for the assay. cGMP content was measured by using the cGMP Enzyme Immunoassay Biotrak System (GE Healthcare, Buckinghamshire, UK) according to the manufacturer's instructions. The test is based on the recognition of cGMP by specific antibodies. cGMP present in the sample and cGMP-enzyme-conjugate compete for the binding sites of the antibodies immobilized on the well plate. Control slices were treated with the vehicle alone, which had no effect on this assay at the final concentration (1 %).

Materials

MK-801 was purchased from Sigma Chemical Co. (St. Louis, MO, USA). WST-1 was obtained from Roche Diagnostics (Indianapolis, IN, USA). cGMP Enzyme Immunoassay Biotrak System was obtained from GE Healthcare (Buckinghamshire, UK). All other chemicals were obtained from Nacalai Tesque Inc. (Kyoto, Japan).

Statistical analysis

The presented values are shown as mean ± SD. The Kolmogorov–Smirnov test was used to evaluate differences for significance. $P < 0.05$ was considered statistically significant.

Results

We quantitatively evaluated serial changes in regional CMRglc when ammonia (10 mM) was loaded in the

bathing solution at 200 min. Patlak plots at 30-min intervals in cerebellum when ammonia was loaded are presented in Fig. 1. The graphs indicate that the slope (=k_3*), reflecting the fractional rate constant for phosphorylation of [^{18}F]FDG, was significantly increased by ammonia as compared to that of the unloaded control ($p < 0.05$). Similar results were obtained in cerebral cortex and striatum (Fig. 1; Table 1).

We investigated the effect of pre-treatment with MK-801 (100 μM) on the slope (=k_3*) after ammonia loading. In cerebellum, MK-801 significantly attenuated the increase in k_3* induced by ammonia loading ($p < 0.05$: significantly different from ammonia group) (Fig. 1; Table 1). A similar effect was not obtained in cerebral cortex or striatum (Fig. 1; Table 1). MK-801 alone had no significant effect on [^{18}F]FDG uptake (Table 1).

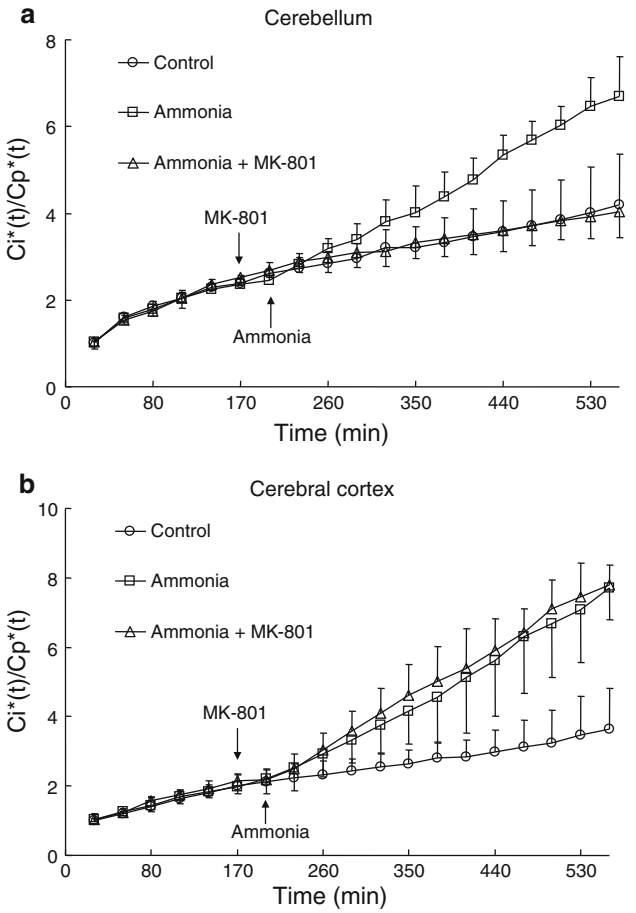

Fig. 1 Effects of 10 mM ammonia loading on the Gjedde–Patlak plots of [^{18}F]FDG uptake in **a** cerebellum and **b** cerebral cortex of rat brain slices. Ammonia was added alone or with the NMDA receptor antagonist MK-801. Ordinate: [Ci*(*t*)/Cp*(*t*)] expressed in terms of the radioactivity signal ratio. Abscissa: time in min indicating $\left[\int_0^t \mathrm{Cp}^*(\tau)\mathrm{d}\tau/\mathrm{Cp}^*(t)\right]$ (see text for further explanation). Time zero is when [^{18}F]FDG was added to the bathing medium containing brain slices. The point at which each agent was added is indicated by an *arrow*. Values are mean ± SD obtained for six slices (SD is shown only for the uppermost or lowermost lines)

In the WST-1 colorimetric assay, ammonia significantly reduced the production of WST-1-formazan as compared to the unloaded control ($p < 0.05$) in each of the brain regions examined (cerebral cortex, striatum, and cerebellum). In cerebellum, but not in cerebral cortex or striatum, MK-801 prevented the decrease in the production of WST-1-formazan induced by ammonia loading. MK-801 alone had no significant effect on the production of WST-1-formazan (only the data for cerebellum are shown in Fig. 2; the results for all the regions examined are shown in Online Resource 1 in tabular format).

Cyclic guanosine monophosphate measurement revealed that in cerebellum, but not in cerebral cortex or striatum, the addition of ammonia induced a significant increase in cGMP content ($p < 0.05$), which was prevented by the addition of MK-801. MK-801 alone had no significant effect on cGMP content (only the data for cerebellum are shown in Fig. 3; the results for all the regions examined are shown in Online Resource 2 in tabular format).

Discussion

Our data indicate that ammonia increased the slope of the graph (=k_3*), reflecting the fractional rate constant for phosphorylation of [^{18}F]FDG as compared to that of the unloaded control in each of the brain regions examined (cerebral cortex, striatum and cerebellum) (Fig. 1; Table 1). A previous study has shown the fact that k_3* in the compartment analysis of cerebral glucose metabolism reflects hexokinase activity in the rat brain by positron emission tomography with [^{18}F]FDG (Ouchi et al. 1996). Therefore, this is thought to reflect increased glycolysis, compensating for the decrease in aerobic metabolism when oxidative phosphorylation is inhibited by ammonia. This possibility is plausible because ammonia impaired mitochondrial function, as indicated by a reduction in the activity of the mitochondrial succinate-tetrazolium reductase system (Fig. 2). Our results are consistent with previous studies showing that ammonia facilitates cerebral glycolysis through activation of phosphofructokinase, the rate-limiting glycolytic enzyme (Lowry and Passonneau 1966; Sugden and Newsholme 1975), resulting in an increase in CMRglc (James et al. 1972; Aggarwal et al. 1994; Wendon et al. 1994).

Brain tissue from sparse fur (*spf*) mice, a mutant with an X-linked inherited defect of ornithine transcarbamylase that causes ammonia to accumulate in the blood, contains lower levels of high-energy phosphates (Ratnakumari et al. 1992) and shows a progressive decrease in activity of cytochrome *c* oxidase (complex IV) of the mitochondrial

Table 1 Effect of ammonia loading on the fractional rate constant of [^{18}F]FDG

Brain region	Control	Ammonia	Ammonia + MK-801	MK-801
Cerebral cortex	6.90 ± 0.27	19.73 ± 2.86*	13.70 ± 5.60*	7.33 ± 0.45
Striatum	5.69 ± 0.21	14.95 ± 4.68*	16.59 ± 2.31*	5.81 ± 0.50
Cerebellum	4.67 ± 0.31	12.74 ± 1.71*	4.75 ± 0.14**	4.47 ± 0.34

The k_3* (×1,000), indicating the fractional rate constant of [^{18}F]FDG, was obtained from the slope of the regression equation ($y = ax + b$) fitted to Gjedde–Patlak plots using linear regression analysis. $y = Ci^*(t)/Cp^*(t)$ in terms of the radioactivity signal ratio on the imaging plate; x = time (min) after the start of incubation; a = slope of the line; b = intercept. All values are mean ± SD obtained from six slices

* $p < 0.05$: significantly different from the control

** $p < 0.05$: significantly different from ammonia group

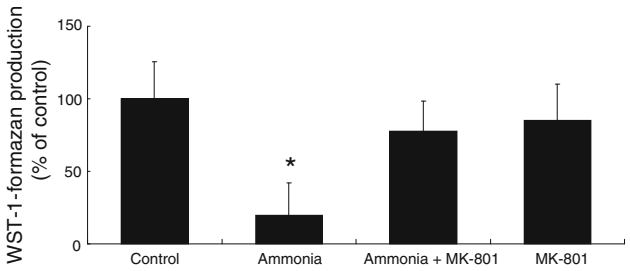

Fig. 2 Effects of ammonia and MK-801 on mitochondrial function in cerebellum of rat brain slices. The WST-1 mitochondrial dehydrogenase assay was performed after pre-incubation with ammonia in the absence or presence of MK-801 for 2 h. The production of WST-1-formazan (product of WST-1 reduction) during the incubation of slices with WST-1 for 3 h (i.e. during the last 3 h of the incubation with ammonia for 5 h) is presented as a percentage of control value. Data represent the mean ± SD obtained for six slices. *$p < 0.05$ compared with control value

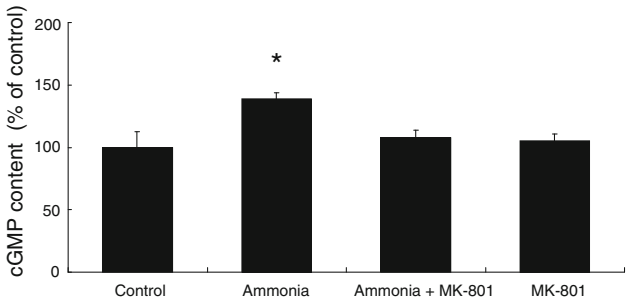

Fig. 3 Effects of ammonia and MK-801 on cGMP in cerebellum of rat brain slices. The increase in cGMP content during the first 5 h after injection of ammonia is presented as a percentage of control value. Data represent the mean ± SD obtained for six slices. *$p < 0.05$ compared with control value

respiratory chain (Rao et al. 1997). Reductions in brain ATP have also been described in adult animals exposed to lethal doses of ammonium salts (McCandless and Schenker 1981; Kosenko et al. 1994). Felipo and Butterworth (2002) proposed two possible mechanisms to explain the deficit in brain energy metabolites in acute hyperammonemia: (i) direct inhibition of αKGDH by the ammonium ion, and (ii) activation of NMDA receptors. In favor of the first mechanism, Lai and Cooper (1986) reported that exposure of brain mitochondria to millimolar concentrations of ammonia in vitro resulted in significant inhibition of αKGDH. Consistent with αKGDH inhibition are the findings of decreased pyruvate oxidation and accumulation of lactate and alanine in brain in acute hyperammonemia (Hawkins et al. 1973; Ratnakumari et al. 1992, 1994).

In cerebellum, ammonia-induced enhancement of glycolysis and impaired mitochondrial function were prevented by NMDA receptor antagonists (Figs. 1, 2; Table 1), which suggest that NMDA receptor activation is responsible for the impairment of glucose metabolism induced by ammonia in this region. This result is consistent with a previous study, which shows that ammonia-induced depletion of ATP is prevented by the administration of NMDA receptor antagonists (Kosenko et al. 1994).

Felipo and Butterworth (2002) proposed two different mechanisms by which NMDA receptor activation contributes to ATP depletion: (i) increased consumption of ATP due to activation of Na^+–K^+-ATPase, and (ii) decreased synthesis of ATP in mitochondria due to impairment of calcium homeostasis. NMDA receptor activation in hyperammonemia results in increased entry of Na^+ and Ca^{2+} into the postsynaptic neuron. Ca^{2+} activates calmodulin, which dephosphorylates and activates Na^+–K^+-ATPase, which in turn extrudes Na^+ and increases ATP consumption. Ammonia-induced increases of Na^+–K^+-ATPase activity are completely prevented by pretreatment with NMDA receptor antagonists (Kosenko et al. 1994; Marcaida et al. 1996). Most of the excess Ca^{2+} is taken up by mitochondria. The consequent impairments of mitochondrial function and generation of reactive oxygen species (ROS) are potentially implicated in the ATP depletion in acute hyperammonemia. Calmodulin that is bound to Ca^{2+} activates NOS, leading to increased generation of ROS. This also contributes to mitochondrial dysfunction and ATP depletion in acute hyperammonemia.

In cerebellum, NMDA receptor antagonists prevented the ammonia-induced rise of cGMP (Fig. 3), which suggests that NMDA receptors are unequivocally activated by

ammonia in this region. This result is consistent with a previous study using in vivo cerebral microdialysis, which found that acute ammonia toxicity led to activation of the NMDA receptor-NO-cGMP signal transduction pathway in brain (Hermenegildo et al. 2000). It is presently unclear how ammonia facilitates NMDA receptor activation. Some argue that inhibition of glutamate uptake is one possibility based on prior studies that illustrate down-regulation of the glutamate transporter GLT-1 and glutamate aspartate transporter GLAST by ammonia (Norenberg et al. 1997; Zhou and Norenberg 1999). However, we believe that this is unlikely because Hermenegildo et al. (2000) reported that the ammonia-induced increase in extracellular glutamate was prevented by a prior injection of MK-801, indicating that the increase in extracellular glutamate is mostly a consequence and not the cause of activation of NMDA receptors (Hermenegildo et al. 2000).

Hermenegildo et al. (2000) proposed that the most likely mechanism underlying ammonia-induced activation of NMDA receptors would be an ammonia-induced depolarization of the neurons. It is well known that the ion channel of NMDA receptors is normally blocked by Mg^{2+} ions in a voltage-dependent manner. Depolarization of the neurons releases the Mg^{2+} blockage, allowing increased activation of the receptors without increasing extracellular glutamate levels (Mayer et al. 1984). A normal concentration of glutamate can activate NMDA receptors when the Mg^{2+} blockage is released by depolarization.

Our results support the idea that, of the three regions analyzed, ammonia-induced activation of NMDA receptors in cerebellum leads to a rise in CMRglc, which is prevented by blocking NMDA receptors (Fig. 1; Table 1). On the other hand, the rise in CMRglc in cerebral cortex and striatum is not a consequence of NMDA receptor activation. The cerebellum has much higher levels of NOS and cGMP than in most brain regions (Steiner et al. 1972; Greenberg et al. 1978; Förstermann et al. 1990), and the dramatic increases in cGMP levels can be seen in response to various drugs in the cerebellum (Ferrendelli et al. 1973; Wood 1991). The increases in cGMP levels in the cerebellum may be largely mediated by NMDA receptor activation, since they could be inhibited by NMDA receptor antagonist (Raiteri et al. 1991). These findings may explain the high activity of the NMDA receptor-NO-cGMP pathway in response to ammonia in the cerebellum. In a ^{1}H magnetic resonance spectroscopy study performed in the rat brain, ammonia injections reduced *N*-acetylaspartate levels, reflecting neuronal damage, in cerebellum but not in substantia nigra. Blocking NMDA receptors prevents the decrease in *N*-acetylaspartate levels in cerebellum (Cauli et al. 2007). These reports may support the idea that NMDA receptor-mediated neurotoxicity in response to ammonia is likely to occur in cerebellum.

Our results indicate that acute ammonia intoxication in cerebral cortex and striatum does not lead to activation of NMDA receptors, and that the rise in CMRglc in these regions is not due to NMDA receptor activation. Although it is presently unclear how ammonia induces the impairment of energy metabolism in cerebral cortex and striatum, there are several plausible mechanisms. First, in detoxification reactions of ammonia, glutamine is formed from glutamate and ammonia using the energy of ATP to drive the synthesis of glutamine, which may result in the loss of ATP (Johansen et al. 2007; Zwingmann 2007). Second, if glutamine is continuously synthesized, neurons will be drained of glutamate and eventually of TCA cycle intermediates (Zwingmann 2007), which may result in the loss of ATP. Third, acute hyperammonemia stimulates NO production by increasing the high affinity transport of the NOS substrate L-arginine (Rao et al. 1995), which suggests a role of the NO signal transduction pathway independent of NMDA receptor-mediated mechanisms.

One of the limitations of our findings is that the ammonia concentration used in this study (10 mM) certainly exceeds physiological blood ammonia concentrations (0.1–0.3 mM, Cooper and Plum 1987) as well as brain ammonia levels reported in models of portal-systemic encephalopathy (3–5 mM, Mousseau and Butterworth 1994). In our preliminary experiment, lower concentrations (less than 10 mM) of ammonia had no significant effect on [^{18}F]FDG uptake, mitochondrial function or cGMP content in each of the brain regions examined (data not shown). However, the concentration level we used (10 mM) is of the same order of magnitude as that in previous in vitro studies (Klejman et al. 2005; Wejksza et al. 2006). The concentration we used may serve to illustrate a general phenomenon that should still hold true even at lower concentrations. Further clarification of the mechanisms involved could be useful in the treatment of patients with hepatic encephalopathy.

In summary, we investigated the effects of acute ammonia loading on cerebral glucose metabolism in the rat brain. Ammonia produced increased glycolysis, compensating for the decrease in aerobic metabolism in each of the brain regions examined (cerebral cortex, striatum, and cerebellum). Ammonia induced the activation of the NMDA receptor-NO-cGMP pathway in cerebellum, but not in cerebral cortex or striatum. Therefore, it is suggested that NMDA receptor activation is responsible for the impairment of glucose metabolism induced by ammonia specifically in cerebellum. Measurements of CMRglc in brain slices using the dPAT may be useful for clarifying the mechanisms underlying ammonia toxicity and the pathogenesis of hepatic encephalopathy.

Conflict of interest All the authors assure that there are no commercial or financial involvements that might present an appearance of a conflict of interest in connection with this article.

References

Aggarwal S, Kramer D, Yonas H, Obrist W, Kang Y, Martin M, Policare R (1994) Cerebral hemodynamic and metabolic changes in fulminant hepatic failure: a retrospective study. Hepatology 19:80–87

Aggarwal S, Obrist W, Yonas H, Kramer D, Kang Y, Scott V, Planinsic R (2005) Cerebral hemodynamic and metabolic profiles in fulminant hepatic failure: relationship to outcome. Liver Transpl 11:1353–1360

Cauli O, López-Larrubia P, Rodrigues TB, Cerdán S, Felipo V (2007) Magnetic resonance analysis of the effects of acute ammonia intoxication on rat brain. Role of NMDA receptors. J Neurochem 103:1334–1343

Cooper AJ, Plum F (1987) Biochemistry and physiology of brain ammonia. Physiol Rev 67:440–519

Felipo V, Butterworth RF (2002) Mitochondrial dysfunction in acute hyperammonemia. Neurochem Int 40:487–491

Ferrendelli JA, Kinscherf DA, Chang MM (1973) Regulation of levels of guanosine cyclic 3′,5′-monophosphate in the central nervous system: effects of depolarizing agents. Mol Pharmacol 9:445–454

Förstermann U, Gorsky LD, Pollock JS, Schmidt HH, Heller M, Murad F (1990) Regional distribution of EDRF/NO-synthesizing enzyme(s) in rat brain. Biochem Biophys Res Commun 168: 727–732

Gjedde A (1981) High- and low-affinity transport of D-glucose from blood to brain. J Neurochem 36:1463–1471

Greenberg LH, Troyer E, Ferrendelli JA, Weiss B (1978) Enzymatic regulation of the concentration of cyclic GMP in mouse brain. Neuropharmacology 17:737–745

Hamacher K, Coenen HH, Stöcklin G (1986) Efficient stereospecific synthesis of no-carrier-added 2-[^{18}F]-fluoro-2-deoxy-D-glucose using aminopolyether supported nucleophilic substitution. J Nucl Med 27:235–238

Hawkins RA, Miller AL, Nielsen RC, Veech RL (1973) The acute action of ammonia on rat brain metabolism in vivo. Biochem J 134:1001–1008

Hermenegildo C, Monfort P, Felipo V (2000) Activation of *N*-methyl-D-aspartate receptors in rat brain in vivo following acute ammonia intoxication: characterization by in vivo brain microdialysis. Hepatology 31:709–715

Huang SC, Phelps ME, Hoffman EJ, Sideris K, Selin CJ, Kuhl DE (1980) Noninvasive determination of local cerebral metabolic rate of glucose in man. Am J Physiol 238:E69–E82

Izumi Y, Izumi M, Matsukawa M, Funatsu M, Zorumski CF (2005) Ammonia-mediated LTP inhibition: effects of NMDA receptor antagonists and L-carnitine. Neurobiol Dis 20:615–624

James IM, MacDonell L, Xanalatos C (1972) The effect of acute portacaval shunting in dogs on cerebral and peripheral blood flow and metabolism. Clin Sci 42:769–774

Johansen ML, Bak LK, Schousboe A, Iversen P, Sørensen M, Keiding S, Vilstrup H, Gjedde A, Ott P, Waagepetersen HS (2007) The metabolic role of isoleucine in detoxification of ammonia in cultured mouse neurons and astrocytes. Neurochem Int 50: 1042–1051

Klejman A, Wegrzynowicz M, Szatmari EM, Mioduszewska B, Hetman M, Albrecht J (2005) Mechanisms of ammonia-induced cell death in rat cortical neurons: roles of NMDA receptors and glutathione. Neurochem Int 47:51–57

Kosenko E, Kaminsky Y, Grau E, Miñana MD, Marcaida G, Grisolía S, Felipo V (1994) Brain ATP depletion induced by acute ammonia intoxication in rats is mediated by activation of the NMDA receptor and Na^+, K(+)-ATPase. J Neurochem 63: 2172–2178

Lai JC, Cooper AJ (1986) Brain alpha-ketoglutarate dehydrogenase complex: kinetic properties, regional distribution, and effects of inhibitors. J Neurochem 47:1376–1386

Lowry OH, Passonneau JV (1966) Kinetic evidence for multiple binding sites on phosphofructokinase. J Biol Chem 241: 2268–2279

Marcaida G, Kosenko E, Miñana MD, Grisolía S, Felipo V (1996) Glutamate induces a calcineurin-mediated dephosphorylation of Na^+, K(+)-ATPase that results in its activation in cerebellar neurons in culture. J Neurochem 66:99–104

Mayer ML, Westbrook GL, Guthrie PB (1984) Voltage-dependent block by Mg^{2+} of NMDA responses in spinal cord neurones. Nature 309:261–263

McCandless DW, Schenker S (1981) Effect of acute ammonia intoxication on energy stores in the cerebral reticular activating system. Exp Brain Res 44:325–330

McKhann GM, Tower DB (1961) Ammonia toxicity and cerebral oxidative metabolism. Am J Physiol 200:420–424

Mousseau DD, Butterworth RF (1994) Current theories on the pathogenesis of hepatic encephalopathy. Proc Soc Exp Biol Med 206:329–344

Murata T, Omata N, Fujibayashi Y, Waki A, Sadato N, Yoshida S, Yano R, Yoshimoto M, Yonekura Y (1999) Dynamic changes in glucose metabolism of living rat brain slices induced by hypoxia and neurotoxic chemical-loading revealed by positron autoradiography. J Neural Transm 106:1075–1087

Norenberg MD, Huo Z, Neary JT, Roig-Cantesano A (1997) The glial glutamate transporter in hyperammonemia and hepatic encephalopathy: relation to energy metabolism and glutamatergic neurotransmission. Glia 21:124–133

Omata N, Murata T, Fujibayashi Y, Waki A, Sadato N, Yoshimoto M, Wada Y, Yonekura Y (2000) Hypoxic but not ischemic neurotoxicity of free radicals revealed by dynamic changes in glucose metabolism of fresh rat brain slices on positron autoradiography. J Cereb Blood Flow Metab 20:350–358

Ouchi Y, Fukuyama H, Matsuzaki S, Ogawa M, Kimura J, Tsukada H, Kakiuchi T, Kosugi T, Nishiyama S (1996) Compartment analysis of cerebral glucose metabolism and in vitro glucose-metabolizing enzyme activities in the rat brain. Brain Res 706: 267–272

Patlak CS, Blasberg RG, Fenstermacher JD (1983) Graphical evaluation of blood-to-brain transfer constants from multiple-time uptake data. J Cereb Blood Flow Metab 3:1–7

Raiteri M, Maura G, Barzizza A (1991) Activation of presynaptic 5-hydroxytryptamine1-like receptors on glutamatergic terminals inhibits *N*-methyl-D-aspartate-induced cyclic GMP production in rat cerebellar slices. J Pharmacol Exp Ther 257:1184–1188

Rao VL, Audet RM, Butterworth RF (1995) Increased nitric oxide synthase activities and L-[^{3}H]arginine uptake in brain following portacaval anastomosis. J Neurochem 65:677–678

Rao KV, Mawal YR, Qureshi IA (1997) Progressive decrease of cerebral cytochrome *c* oxidase activity in sparse-fur mice: role of acetyl-L-carnitine in restoring the ammonia-induced cerebral energy depletion. Neurosci Lett 224:83–86

Ratnakumari L, Qureshi IA, Butterworth RF (1992) Effects of congenital hyperammonemia on the cerebral and hepatic levels of the intermediates of energy metabolism in spf mice. Biochem Biophys Res Commun 184:746–751

Ratnakumari L, Qureshi IA, Butterworth RF (1994) Regional amino acid neurotransmitter changes in brains of spf/Y mice with

congenital ornithine transcarbamylase deficiency. Metab Brain Dis 9:43–51

Sokoloff L, Reivich M, Kennedy C, Des Rosiers MH, Patlak CS, Pettigrew KD, Sakurada O, Shinohara M (1977) The [^{14}C]deoxyglucose method for the measurement of local cerebral glucose utilization: theory, procedure, and normal values in the conscious and anesthetized albino rat. J Neurochem 28:897–916

Steiner AL, Ferrendelli JA, Kipnis DM (1972) Radioimmunoassay for cyclic nucleotides. 3. Effect of ischemia, changes during development and regional distribution of adenosine 3′,5′-monophosphate and guanosine 3′,5′-monophosphate in mouse brain. J Biol Chem 247:1121–1124

Sugden PH, Newsholme EA (1975) The effects of ammonium, inorganic phosphate and potassium ions on the activity of phosphofructokinases from muscle and nervous tissues of vertebrates and invertebrates. Biochem J 150:113–122

Wejksza K, Rzeski W, Turski WA, Hilgier W, Dybel A, Albrecht J (2006) Ammonia at pathophysiologically relevant concentrations activates kynurenic acid synthesis in cultured astrocytes and neurons. Neurotoxicology 27:619–622

Wendon JA, Harrison PM, Keays R, Williams R (1994) Cerebral blood flow and metabolism in fulminant liver failure. Hepatology 19:1407–1413

Wood PL (1991) Pharmacology of the second messenger, cyclic guanosine 3′,5′-monophosphate, in the cerebellum. Pharmacol Rev 43:1–25

Zhou BG, Norenberg MD (1999) Ammonia downregulates GLAST mRNA glutamate transporter in rat astrocyte cultures. Neurosci Lett 276:145–148

Zwingmann C (2007) The anaplerotic flux and ammonia detoxification in hepatic encephalopathy. Metab Brain Dis 22:235–249